

---

# Reconstructing the Initial Relaxation Time of Young Star Clusters in the Large Magellanic Cloud

Simon F. Portegies Zwart<sup>1</sup> and Hui-Chen Chen<sup>1,2</sup>

<sup>1</sup>Astronomical Institute 'Anton Pannekoek' and Section Computational Science, University of Amsterdam, Kruislaan 403, 1098SJ Amsterdam, the Netherlands

<sup>2</sup> Graduate Institute of Astronomy, National Central University, No 300 Jhongda Rd. Jhongli City, Taiwan

**Summary.** We reconstruct the initial two-body relaxation time at the half mass radius for a sample of young  $\lesssim 300$  Myr star clusters in the large Magellanic cloud. We achieve this by simulating star clusters with 12288 to 131072 stars using direct  $N$ -body integration. The equations of motion of all stars are calculated with high precision direct  $N$ -body simulations which include the effects of the evolution of single stars and binaries.

We find that the initial relaxation times of the sample of observed clusters in the large Magellanic cloud ranges from about 200 Myr to about 2 Gyr. The reconstructed initial half-mass relaxation times for these clusters has a much narrower distribution than the currently observed distribution, which ranges over more than two orders of magnitude.

## 1 Introduction

The early evolution of young clusters of stars is of considerable interest because of the rich observational data which became available recently. Studying young star clusters is also important in order to obtain a better understanding of the conditions under which clusters are born. The initial conditions of star clusters have been debated actively over the years, but no consensus has been reached either by observing or simulating the formation process of stellar conglomerates. The main parameters which characterize a star cluster at birth (and any time later) are the number of stars, the mass function and the concentration of the stellar distribution.

Part of the problem in determining the clusters' initial conditions stems from our static view of the universe, our inability to run simulations backward with time and our lack of understanding of the physics of the star(cluster) formation process. In this paper we approach this problem by starting with a series of simulations in which we fix most of the initial conditions but relax

the initial relaxation time. We subsequently calculate the evolution of the star cluster with time. With this series of controlled numerical experiments we trace back the observed parameters for a number of young star clusters in the large Magellanic cloud along parallel trajectories in parameter space.

## 2 Simulations

We focus on young  $t \lesssim 300$  Myr star clusters, because excellent observational data is available for a number of these [1]. For the simulations we adopt the Starlab software environment [2], which acquires it's greatest speed with GRAPE-6 special purpose hardware [3, 4]<sup>1</sup>. Our simulations are performed on the GRAPE-6 hardware at the University of Tokyo and the MoDeStA<sup>2</sup> platform at the University of Amsterdam.

The simulated star clusters are initialized by selecting the number of stars, stellar mass function, the density profile, binary fraction and their orbital elements. For our most concentrated model (simulation #1) we adopt the initial conditions derived by Portegies Zwart et al. [5] to mimic the 7-12 Myr old star cluster MGG-11 in the star-burst galaxy M82. In this paper, however, we extend the evolution of this simulated cluster to about 100 Myr [6]. Subsequent simulations are performed with a larger cluster radius, resulting in a longer initial relaxation time (for details on the simulation models #1-4 with 128k stars as listed in Tab. 1 and see [6]). The stellar evolution model adopted is based on [7], and the binaries are evolved with SeBa [8].

We summarize the selection of the initial conditions for simulation #1c (see Tab. 1, see also [6]): first we selected 131072 stars distributed in a King [9] density profile with  $W_0 = 12$  and with masses from a Salpeter initial mass function ( $x = -2.35$ ) between  $1 M_\odot$  and  $100 M_\odot$ . The total mass of the cluster is then  $M \simeq 433000 M_\odot$ . The location in the cluster where the stars are born is not correlated with the stellar mass, i.e. there is no primordial mass segregation. Ten percent of the stars were randomly selected and provided with a companion (secondary) star with a mass between  $1 M_\odot$  and the mass of the selected (primary) star from a flat distribution. The binary parameters were selected as follows: first we chose a random binding energy between  $E = 10$  kT (corresponding to a maximum separation of about  $1000 R_\odot$ ). The maximum binding energy was selected such that the distance at pericenter exceeded four times the radius of the primary star. At the same time we select an orbital eccentricity from the thermal distribution. If the distance between the stars at pericenter is smaller than the sum of the stellar radii we select a new semi-major axis and eccentricity. If necessary, we repeat this step until the binary remains detached. As a result, binaries with short orbital periods are generally less eccentric. We ignored an external tidal field of the Galaxy, but stars are

<sup>1</sup> see <http://www.astrogrape.org>

<sup>2</sup> see <http://modesta.science.uva.nl>

removed from the simulation if they are more than 60 initial half-mass radii ( $r_{\text{hm}}$ ) away from the density center of the cluster ( $100 r_{\text{hm}}$  for the 12k models, see Tab. 1).

For the other simulations #2c, #3c and #4c, we adopt the same realization of the initial stellar masses, position and velocities (in virial N-body units [10]) but with a different size and time scaling to the stellar evolution, such that the two-body relaxation time ( $t_{\text{rlx}}$ ) for simulation #2c is four times that of #1c, for simulation #3c we used four times the two-body relaxation time of what was used for simulation #2c, etc. the initial conditions are summarized in Tab. 1.

We subsequently generate additional initial realizations for clusters with a smaller number of stars (12k stars for models #\{1..4\}a versus 128k for models #\{1..4\}c). To study the effect of the initial density profile on the results are perform another set of simulations with 12k stars but with a  $W_0 = 6$  initial density profile rather than the highly concentrated  $W_0 = 12$ . The simulations with  $N = 12\text{k}$  are constructed without primordial binaries.

**Table 1.** Conditions for the performed calculations with a range of number of stars ( $1\text{k} \equiv 1024$  stars) and cluster virial radii. The columns give the model name, the number of stars in the initial model, the concentration parameter ( $W_0$ ), the initial half-mass relaxation time ( $t_{\text{rlx}}^i$ ), the initial virial radius and core radius and finally the initial crossing time.

Run	$N$	$W_0$	$t_{\text{rlx}}^i$ [Myr]	$r_{\text{vir}}$ [pc]	$r_{\text{core}}$ [pc]	$t_{\text{ch}}$ [Myr]
#1a	12k	12	73	2.27	0.071	0.258
#1b	12k	6	81	2.77	0.670	0.352
#1c	128k	12	80	1.27	0.010	0.032
#2a	12k	12	304	5.72	0.072	1.05
#2b	12k	6	310	6.98	1.93	1.010
#2c	128k	12	320	3.20	0.026	0.129
#3a	12k	12	1200	14.6	0.151	4.17
#3b	12k	6	1280	17.8	4.28	4.19
#3c	128k	12	1300	8.1	0.066	0.516
#4a	12k	12	4990	36.3	0.317	16.6
#4b	12k	6	4920	44.2	14.9	16.5
#4c	128k	12	5100	20.0	0.162	2.07

After initialization we synchronously calculate the evolution of the stars and binaries, and solve the equations of motion for the stars in the cluster. The calculations are continued to an age of about 100 Myr.

### 3 Results

The main difference between simulations are the number of stars and since we ignore the external tidal field the number of stars drops only slightly during the simulations, but the half-mass relaxation time increasing substantially from its initial value. At the same time the cluster structure changes by becoming less concentrated. The latter is mainly attributed to mass segregation and stellar mass loss (see also [11, 12, 13, 14, 15]). In [6] we compared some of the characteristics of a subset of the here presented simulations with the observed sample of young star clusters in the LMC. Here, in this proceedings paper, we limit ourselves in comparing the currently observed two-body relaxation time and compare these with the results of our simulations.

In figure 1 we present the evolution of the two-body relaxation time at the half-mass radius for the simulated clusters #1{a..c} to #4{a..c}. The relaxation time is roughly constant for the first  $\sim 3$  Myr for simulations #1{a..c}, #2{a..c}, #3c and #4c, to increase at later time. For simulations #3a and #3b the half-mass relaxation time starts to increase only after about 6 Myr, and after about 16 Myr for simulation #4a and #4b. We attribute this effect to the relatively slow response of the latter models, in particular #4a and #4b, to stellar mass loss. For these models mass loss is not adiabatic as is the case for simulations #1 and #2, but rather impulsive (see [16] for a discussion in relation to variations in the orbital parameters of binary star clusters). The later increase in the half-mass relaxation time is mainly caused by stellar mass loss and, in a lesser extend by the internal structural changes resulting from the internal dynamical evolution. The relaxation time for the various simulation models tend to evolve in almost parallel trajectories, with small variations.

We approximate the time evolution of the relaxation time with the following two equations, for the  $N = 12k$  clusters we adopted

$$t_{\text{rlx}}(t) = \left( \kappa t^{2/3} + 1 \right) t_{\text{rlx}}^i. \quad (1)$$

Here  $\kappa = 1/10$  for the 12k models and  $\kappa = 1/6$  for the 128k models. The resulting tracks are presented in Fig. 2.

Since the evolution of the half-mass relaxation time for each set of simulations with the same number of stars behaves quite similar, with an initial offset, we decided to invert Eq. 1 to enable an extrapolation of the initial relaxation time for the observed clusters. The result for the 21 observed clusters with an age  $\lesssim 300$  Myr is presented in Fig. 3. Here we plot our estimate for the initial half-mass relaxation time ( $t_{\text{rlx}}^i$ ) as a function of the measured age of

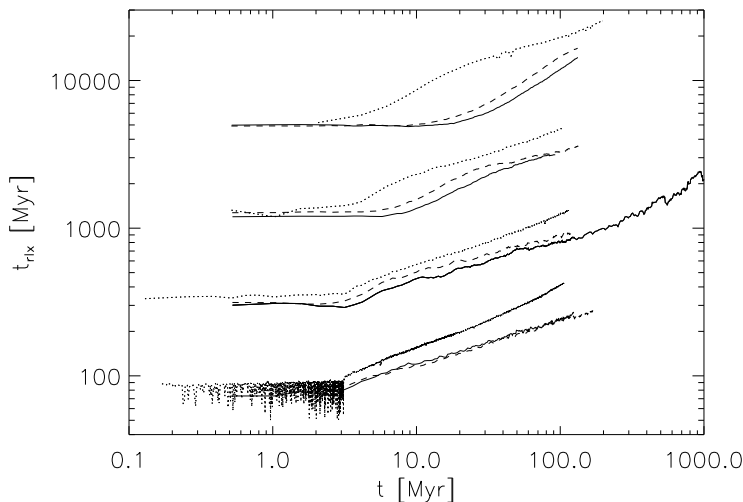


**Fig. 1.** Evolution of the two-body relaxation time at the half mass radius for the four clusters #1 (bottom), #2, #3 and #4 (top). The solid curves represent the data from models #1.4a, dashes give #1.4b and dotted curves gives the results for models #1.4c. Model #2a was extended to an age of 1 Gyr to demonstrate that the generally behavior doesn't suddenly change drastically.

the observed cluster. We ignore the cluster mass in the reconstruction of the initial relaxation times for the observed clusters. From Fig. 1, however, it may be clear that the effect of the number of stars in the cluster is substantial. We therefore opted for having the  $N = 12k$  models to provide an estimate of the upper limit and  $N = 128k$  for providing the lower limit to our estimate of the initial relaxation time. Those lower and upper limits are presented in Fig. 3 as open and filled circles, respectively.

## 4 Discussion and conclusions

We performed extensive simulations of the young star clusters in the large Magellanic cloud. The simulations ignore the external tidal field, and we limited the initial mass function to a Salpeter between  $1 M_{\odot}$  and  $100 M_{\odot}$ . We realize that the adopted initial mass function may not be representative for the large Magellanic cloud, and we performed several additional simulations using the initial mass function proposed by [17], which extends down to the helium burning limit. The difference with the results presented here, however, are quite small, but we tend to underestimate the initial relaxation time compared to using a more realistic initial mass function.

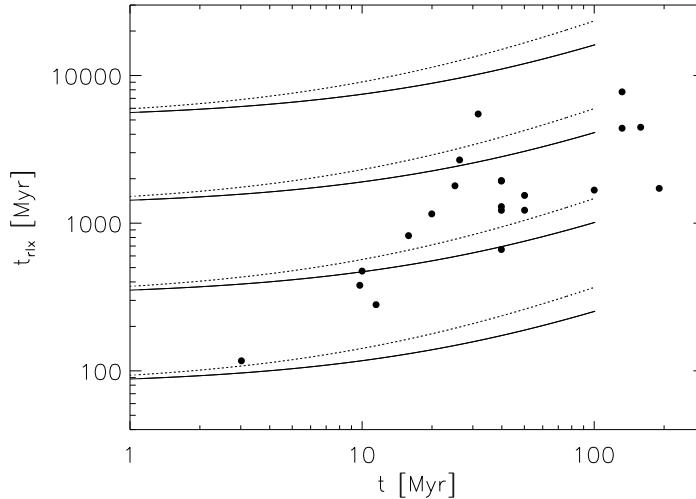


**Fig. 2.** Approximated evolution of the two-body relaxation time at the half mass radius for the four clusters #1 (bottom), #2, #3 and #4 (top). The solid curves represent the data from models with 12k stars (Eq. 1) and dotted curves gives the results for models 128k stars. The bullets give an estimate for  $t_{\text{rx}}$  from the observed clusters [1] by adopting a mean mass of  $0.5 M_{\odot}$  and  $r_{\text{hm}} = 3.92 r_{\text{core}}$ .

The half-mass relaxation time for the simulated clusters evolves on almost parallel trajectories with an initial offset based on the initially selected relaxation time. The trends in the relaxation time is somewhat different from the smaller (in  $N$ ) clusters than for the larger clusters, as is evident in Fig. 1. We attribute this divergence to the difference in the the initial number of stars in these models, in particular since all other parameters were kept as much as possible identical. We note, however, that our simulation with 128k stars were computed with 10% primordial hard binaries, whereas the smaller simulations with 12k stars were computed without primordial binaries. This difference in the initial conditions may attribute to the differences in the evolution of the half-mass relaxation time. To test this hypothesis we performed several additional simulations with 64k stars and no initial binaries. Interestingly, the evolutionary tracks for the half-mass relaxation time for these models is roughly situated between the 12k and the 128k models. Based on these data we argue that the differences we observe between the 12k and the 128k models can be attributed to the differences in the initial number of stars, and that the presence of primordial binaries has little effect. We will discuss these issues in more detail in an upcoming paper *VI* in the *star cluster ecology* series (Portegies Zwart, McMillan & Makino 2006+x {with  $x \in \mathcal{I}; x \geq 1$ }, in preparation).

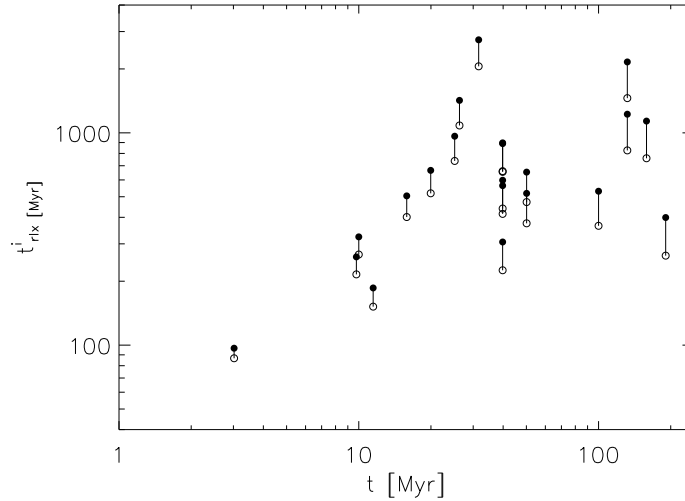


**Fig. 3.** The initial half-mass relaxation time ( $t_{\text{rlx}}^i$ ) as a function of the measured age of the observed LMC cluster. For each cluster we plot two symbols connected with a vertical line. The lower (open circle) symbol indicates extrapolation with time using Eq. 1 for 128k whereas the upper symbols (bullet) gives the result from inverting Eq. 1 for 12k.

Based on the here presented simulations we reconstruct the initial relaxation time for young ( $\lesssim 300$  Myr) star clusters in the LMC with the data from [1]. In Fig. 4 we present the cumulative distribution of initial half-mass relaxation times for the observed star clusters in the LMC. For comparison we overlaid the distribution of the present day relaxation times for the observed clusters, which ranges over more than two orders of magnitude. We conclude that the initial relaxation time for the young ( $\lesssim 300$  Myr) star clusters in the large Magellanic cloud ranges from  $\sim 200$  Myr to  $\sim 2$  Gyr.

## Acknowledgments

I am grateful to Evgenii Gaburov, Mark Gieles, Alessia Gualandris and Henny Lamers for many discussions. This work was supported by NWO (via grant #630.000.001 and #643.200.503), NOVA, the KNAW, the LKBF and the following grants for the Taiwanese government under number NSC095-2917-I-008-006 and NSC 95-2212-M-008-006. The calculations for this work were done on the MoDeStA computer in Amsterdam, which is hosted by the SARA supercomputer center.

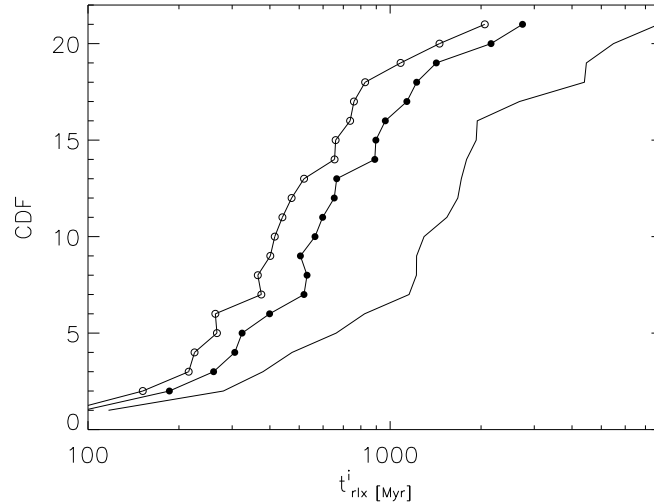


**Fig. 4.** Cumulative distribution of the initial half-mass relaxation time for the observed sample of star clusters in the LMC. The open circles represent the distribution when the initial half-mass relaxation time was reconstructed using the simulations with 128k stars, the filled circles are reconstructed using the 12k simulations. The solid curve without points (to the right) gives the observed distribution of present day relaxation times for the LMC clusters from data published by [1]. We only used the data for those clusters that are younger than 300 Myr.

## References

1. A. D. Mackey, G. F. Gilmore, *MNRAS* **338**, 85 (2003).
2. S. F. Portegies Zwart, S. L. W. McMillan, P. Hut, J. Makino, *MNRAS* **321**, 199 (2001).
3. J. Makino, M. Taiji, T. Ebisuzaki, D. Sugimoto, *ApJ* **480**, 432 (1997).
4. J. Makino, T. Fukushige, M. Koga, K. Namura, *PASJ* **55**, 1163 (2003).
5. S. F. Portegies Zwart, H. Baumgardt, P. Hut, J. Makino, S. L. W. McMillan, *Nature* **428**, 724 (2004).
6. S. Portegies Zwart, S. McMillan, J. Makino, *MNRAS* in press (2006, preprint available at astro-ph/0607461).
7. P. P. Eggleton, M. J. Fitchett, C. A. Tout, *ApJ* **347**, 998 (1989).
8. S. F. Portegies Zwart, F. Verbunt, *A&A* **309**, 179 (1996).
9. I. R. King, *AJ* **71**, 64 (1966).
10. D. C. Heggie, R. Mathieu, *MNRAS* in P. Hut, S. McMillan (eds.), **Lecture Not. Phys 267, Springer-Verlag, Berlin** (1986).
11. D. F. Chernoff, M. D. Weinberg, *ApJ* **351**, 121 (1990).
12. T. Fukushige, D. C. Heggie, *MNRAS* **276**, 206 (1995).
13. S. F. Portegies Zwart, P. Hut, J. Makino, S. L. W. McMillan, *A&A* **337**, 363 (1998).
14. K. Takahashi, S. F. Portegies Zwart, *ApJL* **503**, L49 (1998).



15. H. Baumgardt, J. Makino, *MNRAS* **340**, 227 (2003).
16. S. Portegies Zwart, S. Rusli, *MNRAS* in press (2006, preprint available at astro-ph/0609061).
17. G. de Marchi, F. Paresce, S. Portegies Zwart, in E. Corbelli, F. Palla, H. Zinnecker (eds.), *ASSL Vol. 327: The Initial Mass Function 50 Years Later*, p. 77 (2005).